

Polariton Resonances for Ultrastrong Coupling Cavity Optomechanics in GaAs/AlAs Multiple Quantum Wells

B. Jusserand,¹ A. N. Poddubny,² A. V. Poshakinskiy,² A. Fainstein,³ and A. Lemaitre⁴

¹*Institut des Nanosciences de Paris, CNRS UMR 7588, Université Pierre et Marie Curie (UPMC), 75005 Paris, France*

²*Ioffe Institute, 194021 St. Petersburg, Russia*

³*Centro Atómico Bariloche and Instituto Balseiro, C.N.E.A., 8400 S. C. de Bariloche, R. N., Argentina*

⁴*Laboratoire de Photonique et de Nanostructures, CNRS UPR 20, 91460 Marcoussis, France*

(Received 16 September 2015; published 29 December 2015)

Polariton-mediated light-sound interaction is investigated through resonant Brillouin scattering experiments in GaAs/AlAs multiple-quantum wells. Photoelastic coupling enhancement at exciton-polariton resonance reaches 10^5 at 30 K as compared to a typical bulk solid room temperature transparency value. When applied to GaAs based cavity optomechanical nanodevices, this result opens the path to huge displacement sensitivities and to ultrastrong coupling regimes in cavity optomechanics with couplings g_0 in the range of 100 GHz.

DOI: 10.1103/PhysRevLett.115.267402

PACS numbers: 78.20.hb, 71.36.+c, 78.30.Fs, 78.67.Pt

The field of cavity optomechanics [1] offers a rich variety of novel phenomena and applications, mostly based up to now on the silicon platform in which nanofabrication techniques have reached a very high level of maturity. This technological choice has led to the consideration of essentially a single dominant mechanism for the coupling between optical and mechanical degrees of freedom in micro- or nanoresonators, the so-called radiation pressure. In that case, optical resonances are modified by the surface and interface displacements exclusively. More recently, GaAs has been considered [2,3] as an alternative choice of great potential in relation with the well-established optoelectronic properties of direct gap semiconductors not available in silicon. It was pointed out in Ref. [3] that, in GaAs, radiation pressure has to be combined with a second mechanism, the photoelastic coupling, in order to quantitatively describe optomechanical coupling efficiency in nanomechanical devices based on the GaAs platform. The photoelastic coupling describes the modification of the dielectric properties of the device in the presence of strain fields accompanying the mechanical behavior [4–6].

Cavity optomechanics can thus benefit from an optimization of the photoelastic coefficients in the constituting materials. Contrary to radiation pressure, photoelastic coupling strongly depends on the wavelength of light involved in the experiments and, in particular, on its detuning from intrinsic optical resonances in the material [7]. These resonances can be described either in the excitonic or in the polaritonic picture depending upon experimental conditions such as the temperature, the residual nonradiative damping, or the inhomogeneous broadening of the relevant transitions [8]. As recently proposed, polaritons in cavities could allow access to a fully resonant light-sound interaction regime, avoiding detrimental effects related to dissipation, which is of great

interest for cavity optomechanics [9]. A model for the phenomena, and a determination of the magnitude of this interaction, is, however, still lacking.

Photoelastic coupling in bulk GaAs has been measured in the last decades using standard piezo-optics schemes such as transmission birefringence [10,11] or ellipsometry [12] in the presence of externally applied static stress. These experiments provide useful information either in the transparency region or in the presence of significant absorption, respectively; i.e., they leave the strong resonance domain near the absorption edge fully uncharted. Resonant Brillouin scattering has been demonstrated as a powerful method to study acousto-optical coupling near exciton resonances [13,14]. It has the additional advantage that thermally activated internal strains are involved and usually complex stress apparatus can be avoided. Unfortunately, a quantitative description of the resonant Brillouin scattering cross section including the exciton-polariton range had not been obtained until very recently [15].

Systematic studies of the photoelastic coupling thus emerge as of great interest in the new developing field of GaAs-based cavity optomechanical nanodevices. In this Letter, we show that the analysis of the Brillouin scattering intensity in GaAs/AlAs multiple quantum wells (MQWs) provides a quantitative determination in a large range of temperatures of resonant optical and optomechanical parameters with unprecedented accuracy and completeness as compared to previous piezo-optical experiments [10–12]. We demonstrate huge enhancement of the photoelastic constants of GaAs/AlAs MQWs at resonance and with decreasing temperature, thus opening the way to ultrastrong coupling regimes in cavity optomechanics.

We performed resonant Brillouin backscattering experiments between 30 and 290 K on a very high quality MQW

containing 40 GaAs wells with a thickness of 17.1 nm separated by AlAs barriers of 7.5 nm thickness [15]. With such relatively thick barriers, the electronic states in each quantum well have a negligible overlap with their analogues in neighboring wells. Only radiative coupling between quantum well excitons with nondispersive character along the stacking direction governs their interaction. A MQW is also a periodically modulated acoustic structure so that its acoustic properties can be described in the folding scheme [4]. Acoustic waves with wave vectors shifted by a multiple of the Brillouin minizone extension $2\pi/d$, and frequencies much larger than the standard Brillouin frequency become active for polariton scattering. We have covered the largest possible laser energy range including both the low energy tail of the resonance towards the transparency region and the light-hole exciton range, a few meV above the heavy-hole one. We focus in this Letter on the quantitative analysis of the temperature dependent heavy-hole fundamental exciton polariton resonance which is the strongest and the most relevant for cavity optomechanics applications.

We show in the left panel of Fig. 1 typical Brillouin spectra obtained when the laser energy is very close to the heavy-hole exciton energy (strong resonance) at a few different temperatures using a very narrow and stable tunable laser line and a double spectrometer with a very high resolution close to 0.11 cm^{-1} ($14 \mu\text{eV}$). When the temperature is decreased, the scattering intensity increases

dramatically (not visible in Fig. 1 showing rescaled spectra). It always remains sufficiently intense as compared to both competing excitonic luminescence and the resonant Rayleigh line to allow accurate determinations of the shift, the width, and the intensity of three Brillouin lines at least, both on the Stokes (ST) and the anti-Stokes (AS) sides of the Rayleigh line [16]. They are associated with the unfolded longitudinal acoustic (LA) phonon and the two lowest folded longitudinal acoustic phonons (FLA1 and FLA2). Below 30 K, exciton luminescence strongly increases and the Brillouin lines broaden in such a way that a clear separation of the different signals becomes difficult in the most interesting strong resonance energy range. We will show below that due to polariton mediation, the peak Brillouin linewidth indeed increases at resonance with decreasing exciton damping while the energy range over which the width is modified strongly shrinks.

We show in the middle and right panels of Fig. 1 the variation with incident energy of the shift and the width of the FLA1 line, for temperatures ranging between 30 and 180 K [16]. The measured curves have been shifted vertically to show relative variations around the temperature dependent heavy-hole exciton energy. Two structures are visible in the energy dependence of both the shift and the width of the Brillouin peaks. They reflect the exciton polariton dispersion when either the incident laser energy or the scattered energy become close to the exciton resonance [8]. The temperature dependence reflects the formation of the polariton gap when the temperature is decreased, i.e., when the nonradiative damping is decreased. At 30 K, a strong resonant enhancement of the Brillouin linewidth is observed in a narrow range, with maximum values around 0.8 cm^{-1} . This behavior looks counterintuitive as the nonradiative exciton damping decreases in the same conditions (see the inset in Fig. 2). The Brillouin shift oscillations also become very abrupt. The polaritonic behavior remains visible until 125–150 K, while at 180 K a standard nondispersive behavior with a constant shift and a very small width is recovered. Our understanding of the physics behind these observations is that, as the temperature is decreased, the exciton damping is reduced and one can thus better approach the fully resonant range where the polariton picture with its mode anticrossing plays a critical role. As one enters this fully resonant domain towards the exciton energy, the lines become broader because polariton states with strong exciton weight are accessed, and the Brillouin intensities become small, because the photon strengths are small and thus photons cannot well couple with the polaritons, and the later cannot well escape from the sample. This polariton picture is washed out towards higher temperatures when nonradiative damping broadens the eigenstates, closes the gap, and provides additional scattering channels.

We show in Fig. 2 the intensity variations of the FLA1 Stokes line for all temperatures available in this study. We

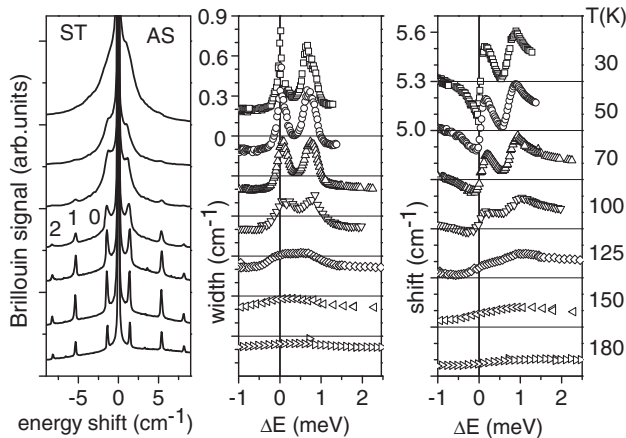


FIG. 1. Left panel: Brillouin backscattering spectra obtained at different temperatures between 30 and 180 K. Intensities have been rescaled and the baselines shifted for clarity. For each temperature, the laser energy coincides with the maximum of the (heavy-hole) exciton line. The lines are labeled 0, 1, and 2 corresponding to the unfolded LA line and the folded FLA1 and FLA2 lines, respectively. Middle and right panel: Variation of the width and the shift of the FLA1 line in the Stokes side plotted as a function of the energy shift relative to the temperature dependent exciton resonance energy (shown with a vertical line). In the center (right) panel, the baseline (a line at 5.3 cm^{-1}) is shown as a thin line for each temperature.

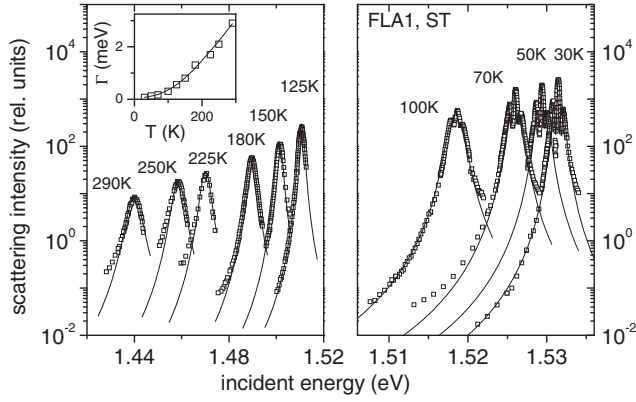


FIG. 2. Variation of the FLA1 line intensity in the Stokes side (FLA1, ST) measured at different temperatures between 30 and 290 K (open squares), plotted as a function of the incident laser wavelength. The latter has been varied around the temperature-dependent exciton resonance. The full lines represent the best fit of the experimental data. The temperature variation of the nonradiative damping parameter (open squares) deduced from the fit is shown in the inset and compared with a simple formula taking into account both the acoustic and LO phonon contributions to the damping (full line).

used the lowest possible laser intensities to measure the resonance behaviors. Values ranged between 10 μ W at low temperature and strong resonance and 2 mW at high temperature. The intensities measured for different temperatures have been carefully normalized to each other and only a global intensity factor common to all data remains arbitrary.

In the same figure, we also show the best fit obtained using the polariton model described in Ref. [15]. In this fit, which provides a comprehensive quantitative description of the measured intensities, all the parameters have been taken constant as a function of the temperature except for the exciton energy and its nonradiative damping. The radiative damping has been taken as 37 μ eV and the nonradiative damping evolution is shown in the inset. It increases regularly with temperature and its value can be remarkably well fitted with a standard formula taking into account a linear contribution associated with the acoustic phonon thermal population and a second contribution proportional to the LO phonon Bose Einstein population (n_{LO}), $\Gamma(T)$ [meV] = 2.4×10^{-3} [meV/K] T + 7.0 [meV] n_{LO} . Both fitted coefficients are in excellent agreement with previous determinations [17,18]. At 30 K the nonradiative contribution to the linewidth becomes as low as 70 μ eV. Quite notably, a negligible constant offset is deduced from the fit, that is $\Gamma(0) = 0$. In contrast, nonvanishing temperature independent contributions have always been deduced from previous experiments, mostly performed on single quantum wells. As we would have assumed a larger contribution in multiple quantum wells due to well fluctuations, our result illustrates both the excellent sample quality and the MQW polariton collective nature. This latter mechanism averages

out, in a similar behavior to motional narrowing [19], the roughness and small layer thickness fluctuations always present in the different quantum wells included in the sample.

Brillouin scattering has been used previously to determine photoelastic coefficients in semiconductors near excitonic resonances, but the measurements remained limited to the transparency side of the resonance [20,21]. Based on the successful quantitative modeling of our measurements over the whole energy range, we extended this concept to our MQW and to the polaritonic description developed in this work. The calculation procedure is outlined below.

The QW photoelastic response is characterized by the tensor $p_{\alpha\beta\gamma\delta}(\omega_i, \omega_s)$ linking the Fourier components of the excitonic polarization $P_\alpha(\omega_s)$, the electric field $E_\beta(\omega_i)$, and the strain tensor $u_{\gamma\delta}(\omega_s - \omega_i)$:

$$4\pi P_\alpha(\omega_s) = -\epsilon_b^2 \int \frac{d\omega_i}{2\pi} p_{\alpha\beta\gamma\delta}(\omega_i, \omega_s) E_\beta(\omega_i) u_{\gamma\delta}(\omega_s - \omega_i). \quad (1)$$

Here, ϵ_b is the QW background dielectric constant. The difference between the incident and scattered wave frequencies $\omega_i - \omega_s$ is due to the absorption (emission) of the longitudinal phonon with the frequency $\Omega = |\omega_s - \omega_i|$. The relevant component of the photoelastic tensor is $p_{12}(\omega) = -(1/\epsilon_b^2)[\partial\epsilon_{xx}(\omega)/\partial u_{yy}]$. It can be extracted from the photoelastic function $p_{\alpha\beta\gamma\delta}(\omega_i, \omega_s)$ as $p_{12}(\omega) = p_{xxyy}(\omega, \omega)$. Brillouin scattering can probe the photoelastic response $p_{12}(\omega)$ as an extrapolation to $\Omega = 0$ of measurements of $p_{12}(\omega_i, \omega_i \pm \Omega)$ at a few different values of Ω . In the vicinity of a QW excitonic resonance ω_0 , the function $p_{12}(\omega_i, \omega_s)$ assumes the form [7]

$$p_{12}(\omega_i, \omega_s) = \frac{4\pi\xi\Gamma_0\Xi(\Omega)}{\epsilon_b^2(\omega_0 - \omega_i - i\Gamma)(\omega_0 - \omega_s - i\Gamma)}, \quad (2)$$

where $\xi = (c\sqrt{\epsilon_b}/2\pi a\omega_0)$ with a being the well width, Γ_0 the exciton radiative decay rate, Γ the nonradiative damping, and $\Xi(\Omega)$ the matrix element of the deformation potential weighted by the overlap integral between the light wave and the phonon mode. Equation (2) is applicable provided that $\Gamma > \Gamma_0$ which is the case even for the lowest considered temperature, $T = 30$ K (where $\Gamma \approx 2\Gamma_0$).

The MQW scattering spectrum $I(\omega_i, \omega_s)$ reads [18]

$$I(\omega_i, \omega_s) = T |t(\omega_i)t(\omega_s)|^2 |\Delta[Q(\omega_i) + Q(\omega_s) - k]|^2 |p_{12}(\omega_i, \omega_s)|^2. \quad (3)$$

The function $\Delta(Q) = \sum_{n=1}^N e^{iQy_n}$ is the structure factor, where the summation runs over the QW positions y_n , $k = \pm\Omega/s$ is the phonon wave vector, where the sign $+$ ($-$) corresponds to the LA, FLA2 (FLA1) modes, respectively. $Q(\omega) = (\omega/c)\sqrt{\epsilon_{\text{eff}}(\omega)}$ is the excitonic polariton wave vector, $t(\omega) = 2q/[q + Q(\omega)]$ is the transmission

coefficient with $q = (\omega/c)\sqrt{\epsilon_b}$, and T is the temperature. The polariton dispersion can be well approximated by the effective dielectric constant $\epsilon_{\text{eff}} = \epsilon_b [1 + \omega_{\text{LT}} / (\omega_0 - \omega - i\Gamma)]$, where ω_{LT} is the longitudinal transverse splitting.

Equation (3) allows us to derive the model parameters based on the simultaneous fit of six different resonant Brillouin intensity variations at each temperature. We show in Fig. 3 two different examples of this fit at the extreme studied temperatures of 30 (left panel) and 290 K (center panel). At 290 K, the fit is excellent. The resonant curves have no structures due to the large nonradiative damping of the exciton at this temperature, which washes out the polariton effects. Nevertheless, even at 290 K the maximum position varies from line to line due to nonzero $\Omega = \omega_i - \omega_s$. At 30 K, the fit remains very good for the folded lines but shows imperfections for the LA line at energies close to the exciton. This could be due to some experimental uncertainties as the exciton luminescence and the resonant Rayleigh line at the laser energy become very intense in these conditions and can perturb the line shape fitting of the LA lines.

We also show in Fig. 3 the calculated static ($\Omega = 0$) intensities based on the same parameters used to fit the

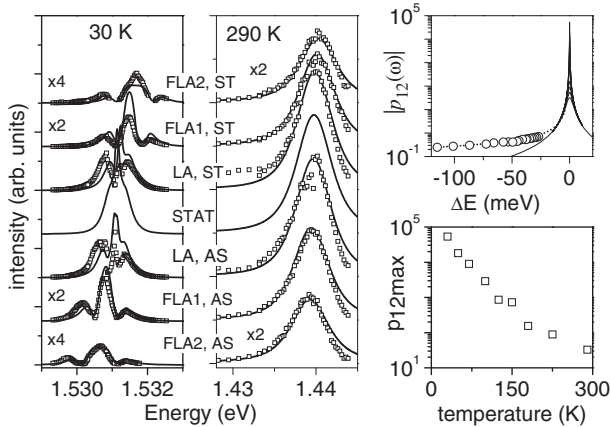


FIG. 3. Variation of the intensity of all Brillouin lines measured at 30 (left panel) and 290 K (center panel), plotted (open squares) as a function of laser energy, around the fundamental exciton resonance (different energy scale for the two temperatures). The continuous curves represent the best fit of the experimental data. The calculated static component ($\Omega = 0$) is also shown in both panels. The top right panel shows with thin lines the modulus of $p_{12}(\omega)$ deduced from our model for all considered temperatures (see text for details). The curve corresponding to 290 K is used to provide an absolute calibration for $p_{12}(\omega)$ by comparison with a previous determination performed at this temperature in the transparency region [11], shown with open circles. To allow for an energy overlap between the two measurements, a theoretical extrapolation of these data towards the exciton energy is also presented (dotted line). Based on this absolute calibration the resulting maximum values of p_{12} at resonance are shown in the bottom right panel for the different temperatures measured (see text for more details).

Brillouin line intensities. They display resonant profiles very similar to the ones for acoustic lines, with somewhat larger peak values due to the superposition of the Stokes and anti-Stokes contributions for $\Omega = 0$. The top right panel shows the static function $p_{12}(\omega)$ deduced with the same approach at all available temperatures. Brillouin scattering provides the modulus of this quantity which is real below the absorption edge but is a complex quantity above it, as it is a strain derivative of the complex dielectric function [22].

To determine the absolute values of the photoelastic response in our sample we have used nonresonant values reported for bulk GaAs in Ref. [11]. Since the contribution of the light hole and the electron-hole continuum to the resonant intensities are quite small as compared to that of the heavy hole, our heavy hole resonance data can be calibrated using the bulk GaAs experiment [11] with a reasonable accuracy. In particular, we extended the model of the photoelastic coefficient presented in Ref. [20] to our strain configuration and applied it to fit the data of Ref. [11] so as to extrapolate its dependence to higher energies. The result is shown by the dotted line in Fig. 3, to be compared with our measurement at 290 K. There is a clear difference between the two curves well below the exciton resonance, a reasonable observation as our model only contains one resonant contribution (that of the heavy hole to conduction electron excitonic transition) and no slowly varying contribution to the dielectric constant from other higher energy optical transitions. As this contribution is very small as compared to the resonant contribution considered in this work (note the logarithmic scale), it is sufficient to consider the range of energy where the two models overlap (-20 to -5 meV typically) to determine the absolute values of the photoelastic modulus at resonance, as derived in our experiment. The lines corresponding to the different measured temperatures in Fig. 3 were obtained with this calibration. The maximum photoelastic constant attained at resonance is displayed as a function of the temperature in the bottom right of Fig. 3. It ranges from 33 to 53 000 between 290 and 30 K. Even when corrected by the GaAs filling factor in the structure, it remains larger by 2 (RT) to 5 (30 K) orders of magnitude as compared to the nonresonant value in GaAs (0.14) used in Ref. [6] to estimate optomechanical coupling in GaAs based nanostructures. As we handle with several orders of magnitude variations as a function of temperature and energy distance to the exciton, this estimation should be accurate enough for future use in the analysis of GaAs MQW optomechanical experiments. Based on the nonresonant values given in Ref. [6] ($p_{12} \sim 0.14$, $g_0 \sim 0.5$ – 2 MHz for different vibrational modes) and the linear scaling [23] of the optomechanical coupling factors g_0 with the photoelastic coefficient p_{12} , the values of g_0 for the obtained photoelastic coefficients $p_{12} \sim 10$ – 10^5 could be expected in the range ~ 0.1 – 100 GHz depending on the experimental temperature.

In conclusion, we have demonstrated huge polariton-mediated resonant enhancement of the photoelastic coupling in GaAs/AlAs MQWs (up to 10^5). We have shown that the resonant Brillouin scattering is a powerful tool that allows the quantitative determination of temperature-dependent photoelastic coupling amplitudes between light and ultrasound in semiconductor nanostructures across excitonic transitions. We have shown that in a GaAs/AlAs multiple quantum well the energy dependence of p_{12} across the heavy-hole exciton resonance can be described within a polariton scattering picture involving three material related parameters only. Our results demonstrate the great advantage to extend nano-optomechanical experiments towards excitonic transition energies with the expected several order of magnitude increase of optomechanical coupling. They give quantitative support to the recent proposals towards a new polariton optomechanics [24,25]. We suggest multiple quantum wells as an excellent option for high sensitivity resonators.

We thank Florent Margailan, Mathieu Bernard, and Silbe Majrab for essential technical support. A. N. P. and A. V. P. acknowledge the support of the Russian Foundation for Basic Research, the Programs of RAS, and the “Dynasty” Foundation.

-
- [1] For a recent review on optomechanics, see M. Aspelmeyer, T. J. Kippenberg, and F. Marquardt, *Rev. Mod. Phys.* **86**, 1391 (2014).
- [2] L. Ding, C. Baker, P. Senellart, A. Lemaître, S. Ducci, G. Leo, and I. Favero, *Appl. Phys. Lett.* **99**, 151117 (2011).
- [3] A. Fainstein, N. D. Lanzillotti-Kimura, B. Jusserand, and B. Perrin, *Phys. Rev. Lett.* **110**, 037403 (2013).
- [4] B. Jusserand, D. Paquet, F. Mollot, F. Alexandre, and G. Le Roux, *Phys. Rev. B* **35**, 2808 (1987).
- [5] V. Gusev, P. Picart, D. Mounier, and J.-M. Breteau, *Opt. Commun.* **204**, 229 (2002).
- [6] C. Baker, W. Hease, D. Nguyen, A. Andronico, S. Ducci, G. Leo, and I. Favero, *Opt. Express* **22**, 14072 (2014).
- [7] B. Jusserand, *Appl. Phys. Lett.* **103**, 093112 (2013).
- [8] B. Jusserand, A. Fainstein, R. Ferreira, S. Majrab, and A. Lemaître, *Phys. Rev. B* **85**, 041302 (2012).
- [9] G. Rozas, A. E. Bruchhausen, A. Fainstein, B. Jusserand, and A. Lemaître, *Phys. Rev. B* **90**, 201302(R) (2014).
- [10] A. Feldman and D. Horowitz, *J. Appl. Phys.* **39**, 5597 (1968).
- [11] P. Renosi and J. Sapriel, *Appl. Phys. Lett.* **64**, 2794 (1994).
- [12] P. Etchegoin, J. Kircher, M. Cardona, C. Grein, and E. Bustarret, *Phys. Rev. B* **46**, 15139 (1992).
- [13] D. K. Garrod and R. Bray, *Phys. Rev. B* **6**, 1314 (1972).
- [14] S. Adachi and C. Hamaguchi, *Phys. Rev. B* **19**, 938 (1979).
- [15] A. N. Poddubny, A. V. Poshakinskiy, B. Jusserand, and A. Lemaître, *Phys. Rev. B* **89**, 235313 (2014).
- [16] See Supplemental Material at <http://link.aps.org/supplemental/10.1103/PhysRevLett.115.267402> for how we extracted the Brillouin lines from the luminescence background and how we fitted their shifts, widths and intensities. The procedures are illustrated for 30 and 50 K when the resonant variations are the strongest.
- [17] T. Ruf, J. Spitzer, V. F. Sapega, V. I. Belitsky, M. Cardona, and K. Ploog, *Phys. Rev. B* **50**, 1792 (1994).
- [18] D. Gammon, S. Rudin, T. L. Reinecke, D. S. Katzer, and C. S. Kyono, *Phys. Rev. B* **51**, 16785 (1995).
- [19] D. M. Whittaker, P. Kinsler, T. A. Fisher, M. S. Skolnick, A. Armitage, A. M. Afshar, M. D. Sturge, J. S. Roberts, G. Hill, and M. A. Pate, *Phys. Rev. Lett.* **77**, 4792 (1996).
- [20] Y. Itoh, S. Adachi, and C. Hamaguchi, *Phys. Status Solidi B* **93**, 381 (1979).
- [21] E. Käräjämäki, R. Laiho, T. Levola, B. H. Bairamov, A. V. Gol'tsev, and T. Toporov, *Phys. Rev. B* **29**, 4508 (1984).
- [22] S. Adachi and C. Hamaguchi, *Phys. Rev. B* **21**, 1701 (1980).
- [23] V. Gusev, P. Picart, D. Mounier, and J.-M. Breteau, *Opt. Commun.* **204**, 229 (2002).
- [24] J. Restrepo, C. Ciuti, and I. Favero, *Phys. Rev. Lett.* **112**, 013601 (2014).
- [25] O. Kyriienko, T. C. H. Liew, and I. A. Shelykh, *Phys. Rev. Lett.* **112**, 076402 (2014).